DNS AND LES OF EXCITED RECTANGULAR JETS

Artur Tyliszczak
Department of Mechanical Engineering and Computer Science, Institute of Thermal Machinery
Czestochowa University of Technology
Al. Armii Krajowej 21, 42-200 Czestochowa, Poland
atyl@imc.pcz.czest.pl

Bernard J. Geurts
Department of Applied Mathematics, Multiscale Modeling and Simulation
University of Twente
P.O. Box 217, 7500 AE Enschede, The Netherlands
B.J.Geurts@utwente.nl

ABSTRACT

The paper presents results of numerical studies devoted to an active flow control method applied to jet flow and focusses on rectangular jets with aspect ratio $A_r = 1,\ 2$ and 3. Square and rectangular jets are more unstable than their circular counterparts, which is expressed by an increased intensity of mixing. It is shown that the application of a suitable excitation (forcing) at the jet nozzle can qualitatively alter the character of the flow, resulting in an increased spreading rate of passive tracer. The excitation is obtained from a superposition of axial and helical forcing terms. We study the mixing in the flow upon varying parameters such as the frequency of the excitations and possible phase shifts between components. The numerical results are obtained applying LES and DNS based on a high-order compact difference code for the incompressible flows.

INTRODUCTION

Interest in flow control techniques is driven by the potential to gain considerable improvement of performance, safety and efficiency of various technical devices. Flow control may be divided into two categories, a passive and an active control (Krall, 1998). The former most often relies on optimisation procedures which are based on geometric shaping or adding fixed elements (obstacles, swirlers, etc.) to the flow domain. Active methods require the input of energy to the flow whose type and level may be constant or may be varying in response to the instantaneous flow behaviour. An evident advantage of passive flow control is its low cost. However, modifications to the flow domain can not be easily adapted to different flow conditions - from this point of view active flow control is much more flexible.

Fundamental research is conducted presently into both flow control techniques. A prominent example of successful alteration of flow dynamics by flow control is the class of jet flows. In these cases the research on passive control techniques concentrates on geometrical modifications of the jet nozzle. It turns out that non-symmetric jets emanating from rectangular or elliptical nozzles enhance mixing between the jet and the surrounding flow. Particularly, the large-scale mixing of non-symmetric jets was found substantially larger than in case of classical circular jets. A comprehensive discussion of the theoretical issues related to non-circular jets and a review of their possible applications may be found in Gutmark and Grinstein (1999).

Concerning active control methods for jet flow most of the research is devoted to circular jets. The work of Crow and Champagne (1971) was probably the first in this category. It was reported that for properly chosen forcing (excitation) frequency the jet behaviour changes qualitatively. An enhanced mixing and the existence of two maxima in the turbulence intensity was found, not seen in the natural jets. The research of Crow and Champagne (1971) initiated many experimental studies which revealed the large potential of active control techniques. A spectacular example of a modified flow pattern is the bifurcating jet which shows the jet splitting in two separate well defined streams (Reynolds et al., 2003).

In this paper we combine active and passive flow control techniques and analyse the resulting flow field. Emphasis is put on alteration of the spreading rate of rectangular jets in conditions of bifurcation. The analysis is performed using DNS (Direct Numerical Simulation) and LES (Large Eddy Simulation). The bifurcation phenomenon is well studied for circular jets (see Danaila and Boersma, 2000; Hilgers and Boersma, 2001; Freund and Moin, 2000; da Silva and Metais, 2002). In contrast, non-circular jets have been much less studied. The existence of enforced bifurcation in rectangular jets was shown by Gohil et al. (2010) and Tyliszczak and Geurts (2012). These studies focussed on qualitative aspects. In this paper we extend this study and quantify the effect of bifurcation in rectangular jets.

GOVERNING EQUATIONS

We consider the incompressible flow described by continuity and the Navier-Stokes equations. In the framework of LES we have:

$$\frac{\partial \overline{u}_j}{\partial x_j} = 0 \tag{1}$$

$$\frac{\partial \overline{u}_i}{\partial t} + \frac{\partial \overline{u}_i \overline{u}_j}{\partial x_j} = -\frac{1}{\rho}\frac{\partial \overline{p}}{\partial x_i} + \frac{\partial \tau_{ij}}{\partial x_j} + \frac{\partial \tau_{ij}^{sgs}}{\partial x_j} \tag{2}$$

where u_i are the velocity components, p - pressure, ρ - density. The overbar denotes spatially filtered variables: $\bar{f}(\vec{x},t) = G * f$ with G being the filter function (Geurts, 2003; Sagaut, 2001). The stress tensor of the resolved field, τ_{ij}, and unresolved subgrid stress tensor τ_{ij}^{sgs} due to filtering of the non-linear advection terms, are:

$$\tau_{ij} = \nu\left(\frac{\partial \overline{u}_i}{\partial x_j} + \frac{\partial \overline{u}_j}{\partial x_i}\right),\ \tau_{ij}^{sgs} = \left(\overline{u}_i\overline{u}_j - \overline{u_i u_j}\right) \tag{3}$$

where ν is the kinematic viscosity. The subgrid tensor is modelled by an eddy-viscosity model with $\tau_{ij}^{sgs} = 2\nu_t S_{ij} - \tau_{kk}\delta_{ij}/3$. The sugbrid viscosity ν_t is computed using the model proposed by Vreman (2004):

$$\nu_t = C\sqrt{\frac{B_\beta}{\alpha_{ij}\alpha_{ij}}} \tag{4}$$

$$\alpha_{ij} = \frac{\partial \overline{u}_j}{\partial x_i} \quad , \quad \beta_{kl} = \Delta^2 \alpha_{mk}\alpha_{ml} \tag{5}$$

$$B_\beta = \beta_{11}\beta_{22} - \beta_{12}^2 + \beta_{11}\beta_{33} - \beta_{13}^2 + \beta_{22}\beta_{33} - \beta_{23}^2 \tag{6}$$

This model yields zero eddy-viscosity close to a solid wall in laminar flows or in pure shear regions. This is very important in jet flows where turbulence develops in the shear layer region.

SIMULATION PARAMETERS

The computational domain together with the nozzle is presented in Fig. 1. In the present work we simplify the problem and do not consider the geometry of the nozzle. Hence, our domain is a simple rectangular box which starts in the plane of the nozzle exit. Its dimensions are $12D \times 16D \times 12D$ where D is the nozzle width along its minor axis. The inlet boundary conditions are specified in terms of the mean velocity profile superimposed with fluctuating components. Outside the jet region a small co-flow is added in order to mimic the natural suction. At the lateral boundaries the streamwise velocity (in the main jet direction) is assumed equal to the co-flow velocity and the remaining velocity components are equal to zero. The pressure at the inlet and side boundaries is computed from the Neumann condition $\partial p/\partial n = 0$. At the outlet plane all velocity components are computed from a convective boundary condition $\partial u_i/\partial t + C\partial u_i/\partial y = 0$ with C the convection velocity which is computed at every time step as the mean velocity in the outlet plane. The pressure at the outflow is assumed constant.

Forcing method

In physical experiments the excitation at the nozzle exit is usually produced by a membrane or loudspeaker located upstream of the nozzle or by a mechanical forcing obtained by specially designed flap actuators placed at the nozzle lip (Suzuki et al., 2004). These excitations change the velocity and direction of the flow leaving the nozzle. In the present study we do not consider the geometry of the nozzle and hence the excitation is introduced in a simplified manner by adding the excitation as a component of the velocity prescribed at the inlet. Hence, the inlet velocity profile used in the present work is defined as:

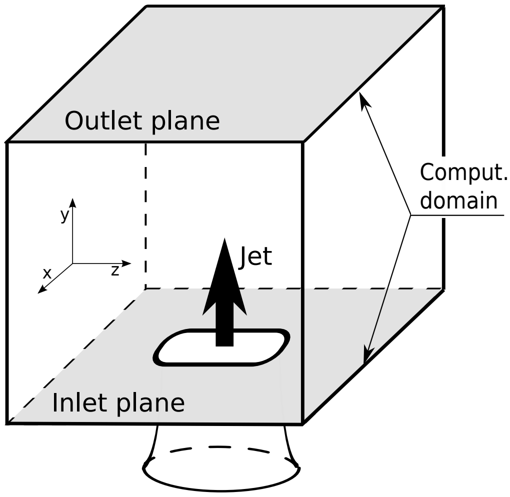

Figure 1. Schematic view of the computational domain.

$$u(\vec{x},t) = u_{mean}(\vec{x}) + u_{excit}(\vec{x},t) + u_{turb}(\vec{x},t) \tag{7}$$

where the mean velocity is a hyperbolic-tangent profile:

$$u_{mean}(\vec{x}) = U_c + \frac{U_{jet}}{4}\left[1 - \tanh\left(\frac{1}{4}\frac{R_x}{\theta}\left(\frac{x}{R_x} - \frac{R_x}{x}\right)\right)\right] \times \left[1 - \tanh\left(\frac{1}{4}\frac{R_z}{\theta}\left(\frac{z}{R_z} - \frac{R_z}{z}\right)\right)\right] \tag{8}$$

Here U_{jet} and U_c denote the jet centerline velocity and the co-flow, respectively. The symbols x, z are the in-plane coordinates, $R_x = D/2$ and $R_z = H/2$ are the nozzle half width of the minor and major axes. The paramer θ is the momentum thickness of the initial shear layer. In all cases presented the shear layer thickness of the jet is characterised by $\theta = R_x/20$. The forcing component $u_{excit}(\vec{x},t)$ is added to the streamwise velocity only:

$$u_{excit}(\vec{x},t) = A_a \sin\left(2\pi St_a \frac{U_{jet}}{D} t\right) + \tag{9}$$

$$+A_h \sin\left(2\pi St_h \frac{U_{jet}}{D} t + \phi\right) \sin\left(\frac{\pi x}{R_x}\right) \tag{10}$$

which is the superposition of axial forcing with amplitude A_a and helical/flapping forcing with amplitude A_h, shown schematically in Fig. 2. The Strouhal numbers are defined as $St_a = f_a D/U_{jet}$ and $St_h = f_h D/U_{jet}$ where f_a, f_h are the frequencies of the axial and helical excitation. The symbol ϕ is the phase shift between axial and helical forcing.

The turbulent fluctuations $u_{turb}(\vec{x},t)$ are computed applying a digital filtering method proposed by Klein et al., (2003). This method guarantees spatially correlated velocity fields which can be tuned to reflect real turbulent flow conditions. Combined, the forcing of the flow can be used to manipulate the main mixing properties (Geurts, 2001; Kuczaj and Geurts, 2006).

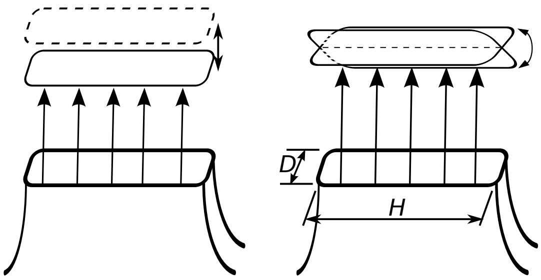

Figure 2. Schematic view of the forcing terms: axial - left side figure and helical on the right hand side.

LES/DNS solver

The LES/DNS solver used in this work is an academic high-order code SAILOR which was used previously in various studies, including laminar/turbulent transition in free jet flows (Tyliszczak et al., 2008), multi-phase flows (Aniszewski et al., 2012) and flames (Tyliszczak, 2013). The SAILOR code is based on a projection method with time integration performed by a predictor-corrector (Adams-Bashforth / Adams-Moulton) method. The spatial discretization is based on the 6th order compact difference method developed for half-staggered meshes (Laizet and Lamballais, 2009). LES and DNS are performed with exactly the same numerical schemes. In the latter case the subgrid viscosity is set to zero and the computational meshes are significantly denser.

NUMERICAL RESULTS

We analyse jets with aspect ratios equal to $A_r = H/D =$ 1, 2 and 3 where D and H are the dimensions of the virtual nozzles shown in Fig. 2. We focus on the influence of the excitation parameters on the spreading rate and emphasize conditions displaying jet bifurcation. In round jets it has been observed that bifurcation occurs in a wide range of Reynolds numbers. Experiments as well as DNS and LES of round jets showed existence of a bifurcation for $1.5 \times 10^3 < Re < 10^5$. Moreover, it was found that the flow is only weakly dependent on Re. Necessary conditions leading to a bifurcation were formulated in terms of forcing frequencies (Reynolds et al., 2003) yielding a Strouhal criterion $St_a/St_h = 2$ with $0.35 < St_a < 0.7$ being close to the preferred mode frequency. In the present work simulations are performed for Reynolds number $Re = 3200$ and $Re = 10000$. We included $Re = 3200$ to compare with earlier work of Grinstein et al. (1995), simulating a subsonic square jet at Mach number equal to 0.3. This validation step preceded studies with varying excitation parameters. Table 1 summarises all computational cases analysed in this work. In all the simulations the excitation amplitudes were assumed equal to $A_a = A_h = 0.15$, similarly as in Danaila and Boersma (2000) for helically forced round jets.

Natural, non-excited jets

The first set of simulations was performed at $Re = 3200$ for the square jet with aspect ratio $A_r = 1$ without excitations. Five different grids were used with sizes as given in Table 2. Figure 3 shows profiles of the mean and RMS axial velocity along the jet axis, while Figure 4 displays the radial distribution of the RMS velocity at $y/D = 7$. Clearly, the results obtained with DNS and LES are very similar at the chosen spatial resolutions. In the present simulations the term DNS basically reflects LES without subgrid model rather than true DNS where all flow scales are fully resolved. The condition that all scales are properly resolved was not systematically underpinned with significantly higher resolutions. However, since a high order spatial discretization method was used and the results denoted as DNS show only a weak mesh dependence at the higher resolutions, it appears that the relevant dynamic flow scales determining mean and RMS velocity are correctly resolved.

Table 1. Computational cases, specified by aspect ratio A_r, Reynolds number Re, axial and helical Strouhal numbers St_a, St_h and phase difference ϕ.

Cases	A_r	Re	St_a	St_a/St_h	ϕ
C1	1	3200	0.4	2	0
C2	1	10^4	0.3-0.6	2	$0, \frac{\pi}{4}$
C3	1, 2, 3	10^4	0.4	1,3,4	$0, \frac{\pi}{4}$
C4	2, 3	10^4	0.5, 0.6	2	$0, \frac{\pi}{4}$

Table 2. DNS/LES mesh parameters.

Re	DNS	LES
	$160 \times 256 \times 160$	$128 \times 160 \times 128$
3200	$160 \times 320 \times 160$	$160 \times 256 \times 160$
	$256 \times 320 \times 256$	
	–	$128 \times 160 \times 128$
10000	–	$160 \times 256 \times 160$
	–	$256 \times 320 \times 256$

The results of LES obtained on the denser mesh appear very close to DNS. Nearly perfect agreement is observed with DNS for the mean and RMS velocity. In this case the LES subgrid flux appears not to contribute much to the dynamics. From Figure 4 it is seen that at $160 \times 256 \times 160$ nodes the LES results are slightly better than the corresponding "pseudo DNS" solution. LES on the coarser mesh is slightly less accurate, underestimating the turbulent fluctuations while the potential core is somewhat overestimated.

Excited jets

At $Re = 3200$ (case C1) the excited jet clearly shows the existence of a bifurcated jet both in DNS and LES. This may be seen in Figure 5 showing contours of mean axial velocity in an $x - y$ plane in Figure 1). Starting from $y/D \approx 5$ the jet divides symmetrically into two branches, whereas the flow in the central part vanishes. A general agreement between DNS and LES is observed also on the coarsest mesh, despite the fact that the LES results show slightly larger spreading of the jet branches. Also at $Re = 10000$ the

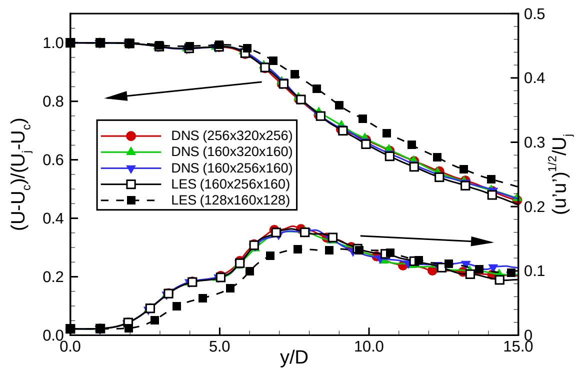

Figure 3. Profiles of the mean and fluctuating component of the axial velocity along the jet axis for DNS and LES simulations, ($Re = 3200$, square jet: $A_r = 1$).

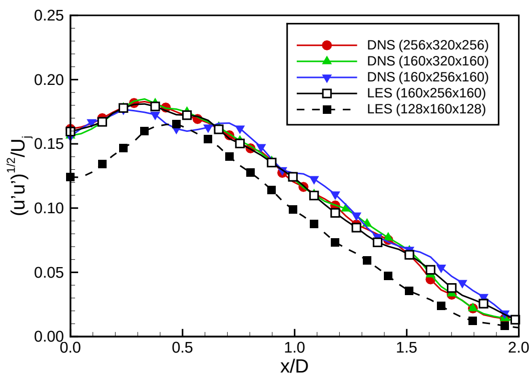

Figure 4. Profiles of the fluctuating component of the axial velocity along the radial direction at $y/D = 7$ for DNS and LES simulations, ($Re = 3200$, square jet: $A_r = 1$).

same general agreement was established using a mesh with $128 \times 160 \times 128$ nodes capturing the larger scales in the flow. This allows to perform a systematic parameter study for the various excitation parameters at acceptable computational costs. In the sequel LES results are presented as obtained on the coarsest mesh.

Figure 6 shows isosurfaces of the instantaneous vorticity modulus on top of contours of the mean axial velocity obtained in computations of jets with aspect ratio $A_r = 2$ at $Re = 10000$. In the excited case the parameters were: $St_a = 0.4$, $St_a/St_h = 2$ and $\phi = 0$. This is seen to yield a jet bifurcation, as also observed in Gohil et al. (2010). The results in Figure 6 are presented in view along the major axis (upper figures) and along the minor axis (lower figures). Thus the velocity contours are presented both in the bifurcation plane and in the so-called bisection plane. For the non-excited jet the potential core region extends to $3.0-3.5\ D$, beyond which the jet spreads radially with a higher intensity along the minor axis. In fact, at $y/D \approx 5$ the jet dimensions along the two axes become equal - this is the so-called crossover point and its location agrees well with data given in Gutmark et al. (1999).

The effect of forcing is readily noticed for the excited jet. There is no potential core region and very strong vortical structures are seen immediately downstream of the inlet, resembling deformed toroidal rings due to the axial forcing. Careful inspection of Figure 6 allows identifying so-called hairpin vortices originating from the corners, with

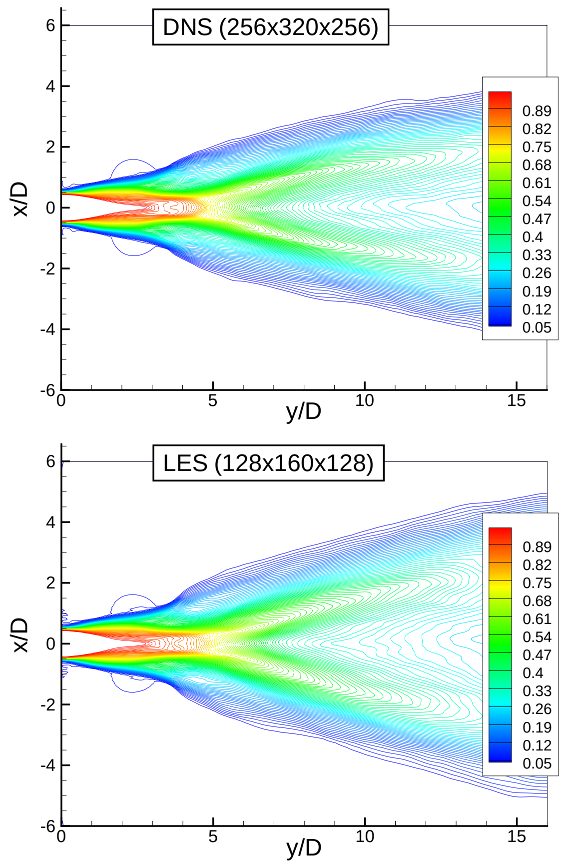

Figure 5. Mean axial velocity contours of the excited jet with aspect ratio $A_r = 1$. Up: DNS; down: LES results.

elongated shapes. The effect of the helical forcing is not as pronounced and its influence starts to be seen only after some distance from the inlet, i.e., beyond $y/D \approx 7$. Helical forcing manifests itself by the division of the main stream in two branches and a deflection of these branches. As could be seen in Figure 5 the angle of the deflection remains basically constant beyond the bifurcation location. The spreading of the jet in the bifurcating plane is considerably larger than in the bisecting plane. The results obtained for circular jets (Hilgers and Boersma, 2001) showed that jet is strongly influenced by the forcing frequency St_a. In case of a rectangular jets the influence of St_a appears even stronger.

Surprisingly, for the rectangular jet also the phase shift between the axial and helical forcing components plays an important role - it may even change the flow behaviour qualitatively. Figures 7-9 show the radial profiles of the mean axial velocities for the selected cases from series C3 and C4 (Table 1). These profiles were extracted from the bifurcation plane at locations $y/D = 3$ and $y/D = 11$. Compared to the non-excited jets (solid lines) the spreading rate of the excited jets increases, regardless of St_a and ϕ. Concerning the existence of a jet bifurcation the situation is less clear. We consider a jet bifurcation to occur when the mean velocity at the axis (i.e., $x/D = 0$) is smaller than at any other locations (i.e.,$x/D \neq 0$). From figures 7-9 it is seen that the forcing frequency and the phase shift affect the flow field differently depending on the jet aspect ratio. For $A_r = 1$ the bifurcation is seen to occur for all St_a, provided $\phi = 0$, whereas with $\phi = \frac{\pi}{4}$ the solutions do not differ qualitatively from the non-excited jet. The situation changes for $A_r = 2$; a jet bifurcation is observed only for the excitation with $St_a = 0.4, \phi = 0$.

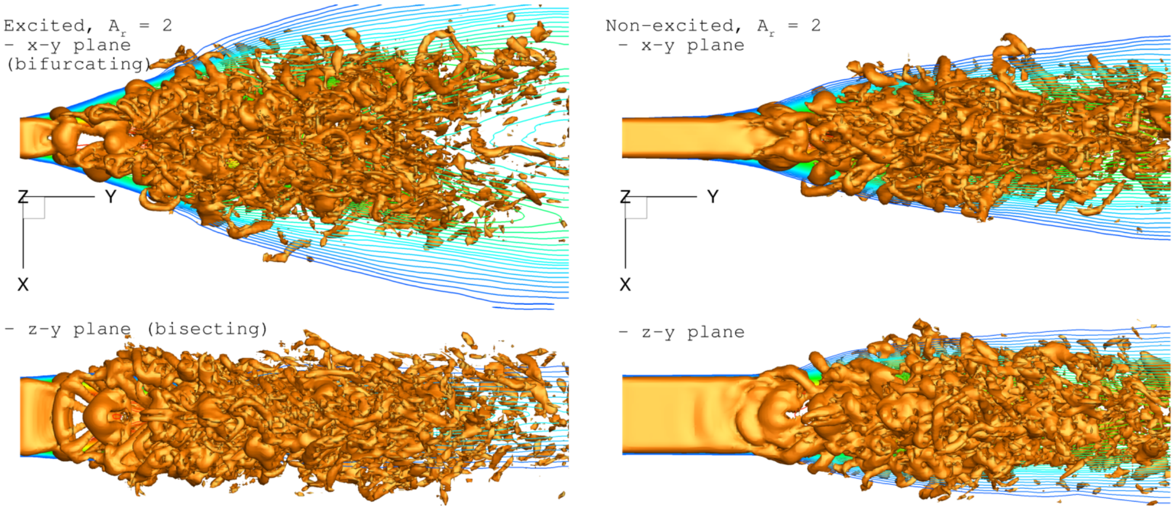

Figure 6. Vorticity isosurface and contours of time averaged axial velocity for the jet with aspect ratio $A_r = 2$. Left figures: excited jet in the x-y (up) and z-y plane (down). Right figures: non-excited jet in the x-y (up) and z-y plane (down).

For $A_r = 3$ the flow behaviour alters even more - in this case for $\phi = 0$ the solutions for all St_a are similar, whereas for $\phi = \frac{\pi}{4}$ they are significantly different with a jet bifurcation appearing for $St_a = 0.4,\ 0.5$. This rather surprising result shows the complexity of the excited jet flow. At the present time the origin of such qualitative flow transitions could not be explained. It may be related to axes switching observed for natural vortex bifurcation in rectangular jets with larger aspect ratios (Gutmark et al.,1999).

Acknowledgment. This work has been partially supported by the Polish National Science Center under grant DEC-2011/03/B/ST8/06401. Computations have been carried out at SARA Computing Centre (Amsterdam) under grant SH-061, and at Cyfronet Computing Centre (Krakow) within the PL-Grid infrastructure.

REFERENCES

Aniszewski W., Boguslawski A., Marek M. & Tyliszczak A. 2012 A New Approach to Sub-grid Surface Tension for LES of Two-phase Flows. *Journal of Computational Physics* **231**, 7368–7397.

Crow S.C. & Champagne F.H. 1971 Orderly structure in jet turbulence. *Journal of Fluid Mechanics* **48**, 547–691.

Danaila I. & Boersma B.J. 2000 Direct numerical simulation of bifurcating jets. *Physics of Fluids* **12** (5), 1255–1257.

Freund J.B. & Moin P. 2000 Jet mixing enhancement by high amplitude fluidic actuation. *AIAA Journal* **38** (10), 1863.

Germano M., Piomelli U., Moin P. & Cabot W.H. 1991 A dynamic subgrid scale eddy viscosity model. *Physics of Fluids A* **3**, 1760–1765.

Geurts B.J. 2001 Mixing efficiency in turbulent shear layers. *Journal of Turbulence*, Vol. **2**.

Geurts B.J. 2003 *Elements of Direct and Large-Eddy Simulation*. Edwards Publishing.

Gohil T.B., Saha A.K., Muralidhar K. 2010 Control of flow in forced jets: a comparison of round and square cross sections. *Journal of Visualization* **13**, 141–149.

Grinstein F.F., Gutmark E., Parr T. 1995 Near field dynamics of subsonic free square jets. A computational and experimental study. *Physics of Fluids* **7**, 1483–1497.

Gutmark E.J., Grinstein F.F. 1999 Flow control with noncircular jets. *Annual Review of Fluid Mechanics* **31**, 239–272.

Hilgers A. & Boersma B.J. 2001 Optimization of turbulent jet mixing. *Fluid Dynamic Research* **29**, 345–368.

Klein M., Sadiki A. & Janicka J. 2003 A digital filter based generation of inflow data for spatially developing direct numerical and large eddy simulations. *Journal of Computational Physics* **186**, 652–665.

Kral L.D. 1998 Active flow control technology. Technical brief. ASME Fluids Engineering Division.

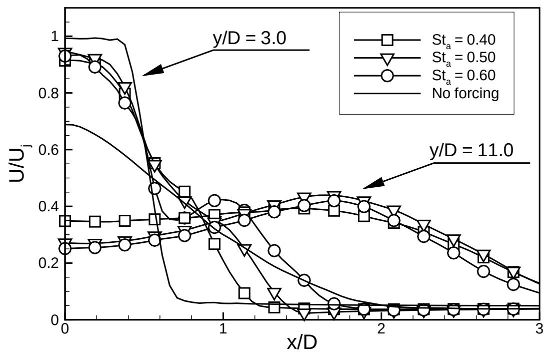

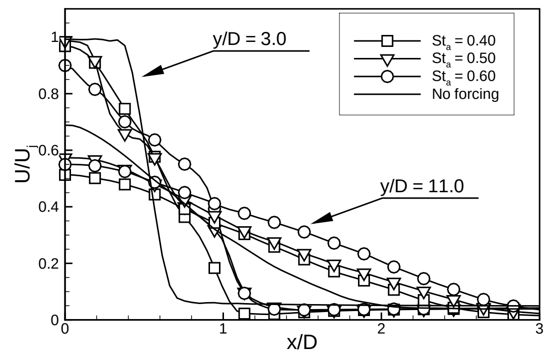

Figure 7. Mean axial velocity profiles for the excited jet with aspect ratio $A_r = 1$. Solutions at $y/D = 3$ and $y/D = 11$ for phase shift $\phi = 0$ (upper figure) and $\phi = \pi/4$ (lower).

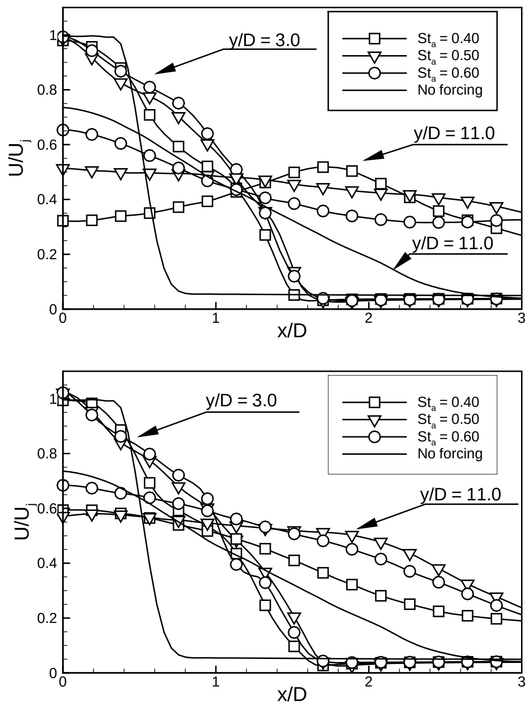

Figure 8. Mean axial velocity profiles for the excited jet with aspect ratio $A_r = 2$. Solutions at $y/D = 3$ and $y/D = 11$ for phase shift $\phi = 0$ (upper figure) and $\phi = \pi/4$ (lower).

Kuczaj A.K., Geurts B.J. 2006 Mixing in manipulated turbulence. *Journal of Turbulence*, Vol. **7**.

Laizet S. & Lamballais E. 2009 High-order compact schemes for incompressible flows: A simple and efficient method with quasi-spectral accuracy. *Journal of Computational Physics* **228**, 5989–6015.

Reynolds W.C., Parekh D.E., Juvet P.J.D. & Lee M.J.D. 2003 Bifurcating and blooming jets. *Annual Review of Fluid Mechanics* **35**, 295–315.

Sagaut P. 2001 *Large eddy simulation for incompressible flows*. Springer.

da Silva C.B. & Metais O. 2002 Vortex control of bifurcating jets: A numerical study. *Physics of Fluids* **14** (11), 3798–3819.

Suzuki H., Kasagi N., Suzuki Y. 2004 Active control of an axisymetric jet with distributed electromagnetic flap actuators. *Experiment in Fluids* **36**, 498–509.

Tyliszczak A. 2013 Assessment of implementation variants of conditional scalar dissipation rate in LES-CMC simulation of auto-ignition of hydrogen jet. *Archives of Mechanics* **65** (2), 97–129.

Tyliszczak A., Boguslawski A. & Drobniak S. 2008 Quality of LES predictions of isothermal and hot round jet. *Quality and Reliability of Large Eddy Simulations, ERCOFTAC Series* **12**, 259–270.

Tyliszczak A., Geurts B.J. 2012 DNS/LES of excited rectangular and round jets. Unpub. presentation of EFM Conference 9.

Vreman A.W. 2004 An eddy-viscosity subgrid-scale model for turbulent shear flow: Algebraic theory and applications. *Physics of Fluids* **16**, 3670–3681.

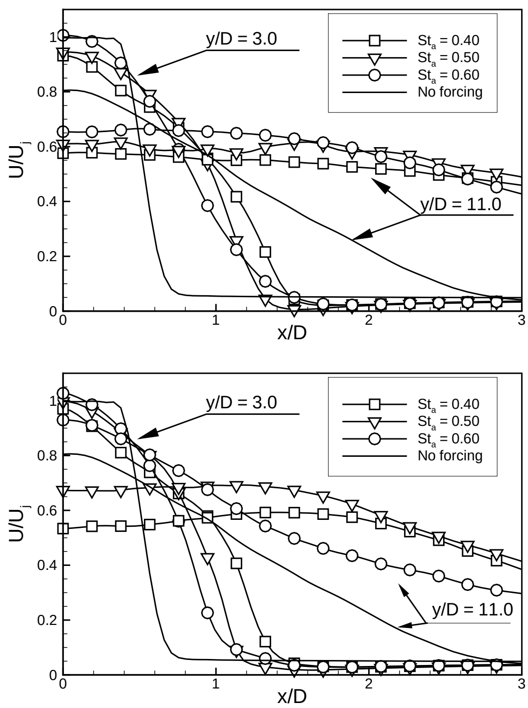

Figure 9. Mean axial velocity profiles for the excited jet with aspect ratio $A_r = 3$. Solutions at $y/D = 3$ and $y/D = 11$ for phase shift $\phi = 0$ (upper figure) and $\phi = \pi/4$ (lower).